Research Article Vol. 6, No. 1 / January 2018 / Photonics Research 1

PHOTONICS Research

Generation of high-energy narrowband 2.05 μm pulses for seeding a Ho:YLF laser

Yanchun Yin, Xiaoming Ren, Yang Wang, Fengjiang Zhuang, Jie Li, and Zenghu Chang*

Institute for the Frontier of Attosecond Science and Technology, CREOL and Department of Physics, University of Central Florida, Orlando, Florida 32816, USA
**Corresponding author: zenghu.chang@ucf.edu*

Received 22 September 2017; revised 31 October 2017; accepted 31 October 2017; posted 3 November 2017 (Doc. ID 307697); published 5 December 2017

We experimentally demonstrate efficient generation of high-energy (82 μJ) narrowband 2.05 μm pulses pumped with 1 mJ broadband Ti:sapphire laser pulses, utilizing dual-chirped optical parametric amplification (DC-OPA) in a BBO crystal. The narrowband 2.05 μm pulses will be primarily used for seeding an Ho:YLF laser, which solves the synchronization issue when Ti:sapphire and Ho:YLF lasers are needed for developing midinfrared lasers. The narrowband 2.05 μm pulse from the unique DC-OPA design can seed the Ho:YLF laser much more efficiently than the broadband 2.05 μm pulse from traditional OPA technology.

OCIS codes: (320.7090) Ultrafast lasers; (190.4410) Nonlinear optics, parametric processes.

https://doi.org/10.1364/PRJ.6.000001

1. INTRODUCTION

Development of high-energy and few-cycle lasers has been of great interest in the ultrafast laser community due to their applications primarily in high harmonic generation (HHG) and attosecond science [1–3]. The shortest (67 as) extreme ultraviolet attosecond pulses have been previously achieved in HHG driven by spectrally broadened few-cycle Ti:sapphire lasers [4]. To extend the HHG cutoff photon energy and thus produce shorter attosecond pulses, long wavelength driving lasers are needed because of the quadratic scaling of the ponderomotive energy with driving wavelength [5–8]. Few-cycle intense infrared (IR) laser pulses around 2 μm have been extensively produced by taking advantage of optical parametric chirped pulse amplification (OPCPA) pumped with few picosecond laser pulses [9–17], dual-chirped optical parametric amplification (DC-OPA) [18–20], and frequency domain OPA [21]. Recently, 53 soft X-ray pulses reaching carbon K-edge were demonstrated by using an mJ-level and two-cycle IR driving laser at 1.7 μm [22].

To significantly increase center photon energy and bandwidth of high harmonics for generating shorter attosecond or even zeptosecond X-ray pulses, the development of high-energy few-cycle pulses farther into the mid-IR is in demand. Rapid progress has been made on the generation of high-energy short-pulse mid-IR laser sources above 3 μm [23–29]. However, the spectral bandwidth has not reached one octave, which limits the pulse duration to multicycle. We have designed a scheme for generation of terawatt subcycle 4–12 μm pulses through OPCPA in $ZGeP_2$ pumped by an Ho:YLF laser [30]. Because the signal of the OPCPA is from a Ti:sapphire laser and the pump is from an Ho:YLF laser, the Ho:YLF laser should also be derived from the Ti:sapphire laser in order to facilitate synchronization between the signal and the pump. In addition, a high-energy seed for the Ho:YLF laser is needed to avoid a regenerative Ho:YLF amplifier—several hundred meters of optical path—that will complicate the synchronization between the Ti:sapphire laser and the Ho:YLF laser. To this end, a high-energy source around 2.05 μm deriving from the Ti:sapphire laser is needed to seed the Ho:YLF laser.

A 2.05 μm laser source with 2 mJ pulse energy has been experimentally demonstrated via traditional OPA [31]. However, the bandwidth from such an OPA is huge compared with the narrow bandwidth of Ho:YLF gain spectrum [32]; thus, the usable energy from the OPA for seeding the Ho:YLF laser would be small. DC-OPA has been first theoretically analyzed [33] and then experimentally demonstrated to generate broadband and tunable wavelength laser sources [18–20,34–36]. Here, in this paper, we designed and experimentally demonstrated the efficient generation of narrowband 2.05 μm pulses pumped with a broadband Ti:sapphire laser via DC-OPA. With 1 mJ Ti:sapphire laser pulses, 82 μJ narrowband 2.05 μm pulses were achieved. The bandwidth and center wavelength can be conveniently tuned around 2.05 μm without losing efficiency to accommodate the gain bandwidth from any Ho:YLF laser [32,37,38].

2. PRINCIPLE OF GENERATING NARROW BANDWIDTH VIA DC-OPA

If there are two input waves in an OPA, the phase of a third output wave will be determined by the phases of the two input waves, thus satisfying the following phase relationship:

$$\phi(\omega_p) - \phi(\omega_s) - \phi(\omega_i) = -\pi/2, \tag{1}$$

in which ω_0 is the central angular frequency, and the subscripts p, s, and i refer to the pump, signal, and idler, respectively. If both the pump and the signal are linearly chirped in a DC-OPA,

$$\omega_{p,s}(t) = \omega_{p0,s0} + \beta_{p,s}t, \tag{2}$$

where β refers to the chirp parameters. By the law of conservation of energy,

$$\omega_i(t) = \omega_p(t) - \omega_s(t) = \omega_{p0} - \omega_{s0} + (\beta_p - \beta_s)t. \tag{3}$$

According to Eq. (3), the chirp of the generated idler is equal to the difference between the pump chirp and the signal chirp. The principle of DC-OPA for generating the narrowband 2.05 μm pulses pumped by broadband Ti:sapphire laser pulses is illustrated in Fig. 1(a). When the broadband pump and the broadband signal have an equal amount of chirp, the frequency difference of all phase-matched pump-signal pairs is a constant and thus generates a single-wavelength idler. This idea has been already proposed and discussed in Refs. [20,33] and has been experimentally demonstrated in Ref. [35]; in the mid-IR region, realization of this scheme is not trivial because it depends on the available phase matching of nonlinear crystals. We found that the narrowband 2.05 μm source can be generated in phase-matching-tailored BBO, as shown in Fig. 1(b). All the pump spectrum (0.76–0.82 μm) and signal spectrum (1.2–1.4 μm) can phase match to generate the idler spectrum around 2.05 μm.

3. SIMULATION RESULTS ON GENERATING NARROW BANDWIDTH VIA DC-OPA

The DC-OPA was simulated using a 1D three-wave mixing numerical model [39] with the following assumptions: (1) the model includes the effects of dispersion; (2) all three waves are collinear and assumed to be plane waves; (3) the gain medium is lossless. The model solves standard coupled differential equations under the slowly varying envelope approximation [40]:

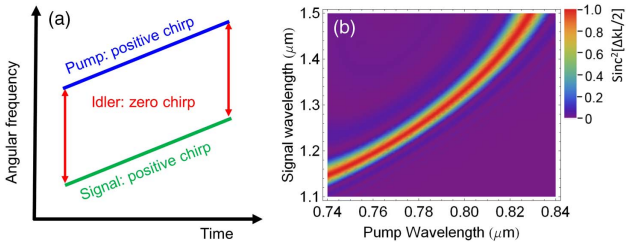

Fig. 1. (a) Illustration of generation of narrowband idler from broadband pump and signal with an equal linear chirp. (b) Normalized phase-matching efficiency of a 10 mm type I (phase-matching angle: 20°) BBO. Δk is the propagation constant difference, and L is the ZGP crystal length.

$$\frac{dA_1}{dz} = j\frac{2d_{\text{eff}}\omega_1^2}{k_1c^2}A_2^*A_3\ \exp(-j\Delta kz), \tag{4}$$

$$\frac{dA_2}{dz} = j\frac{2d_{\text{eff}}\omega_1^2}{k_2c^2}A_1^*A_3\ \exp(-j\Delta kz), \tag{5}$$

$$\frac{dA_3}{dz} = j\frac{2d_{\text{eff}}\omega_3^2}{k_3c^2}A_1A_2\ \exp(j\Delta kz), \tag{6}$$

where $A_{1,2,3}$ are the complex field amplitudes of the signal, idler, and pump waves, respectively, d_{eff} is the effective second-order nonlinearity, ω_i is the angular frequency, k_i is the wave vector, Δk is the wave vector mismatch, c is the speed of light in vacuum, and z is the propagation direction of all three waves. The amplitude and phase of the pump, signal, and idler pulses A_i are represented in the time domain and frequency domain using Fourier transform: $A_i = A_i(t) = F^{-1}[A_i(\omega)]$. The coupled differential equations for the three fields are integrated in the time domain. The dispersion of all three fields are added in the spectral domain using the split-step approach [41] after Fourier transforming the fields into the spectral domain after numerical integration of each step in the time domain. The spectral phase applied to the three fields at each step is

$$A_i(\omega) \rightarrow A_i(\omega)\exp[jn_i(\omega)\omega dz/c], \tag{7}$$

where $n(\omega)$ is the refractive index of the nonlinear medium for the angular frequency ω of wave A_i.

In the simulation, the BBO crystal is 10 mm thick and has a type I configuration with a phase-matching angle of 20.0°. The input pump spectrum spans from 0.75 to 0.85 μm, and the input signal spectrum spans from 1.2 to 1.4 μm, as shown in Fig. 2(a). The input pump and signal intensities are 9 GW/cm^2 and 1 mW/cm^2, respectively. The pump and the signal have a similar input chirp. To study the effects of

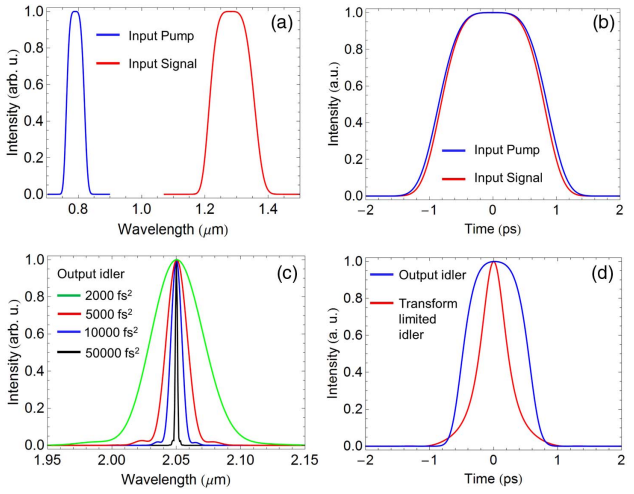

Fig. 2. (a) Input pump (blue) and signal (red) spectra. (b) Input pump (blue) and signal (red) pulse shapes in the case of an initial pump and signal chirp of 10000 fs^2. (c) Output idler spectra under different pump and signal chirps. (d) Output idler pulse shapes in the case of an initial pump and signal chirp of 10000 fs^2 (blue) and transform limited idler pulse shape (red).

pump and signal chirps on the output idler bandwidth, five cases of chirps are considered: 2000, 5000, 10000, and 50000 fs^2. The input pump and signal pulse shapes in the case of 10000 fs^2 are shown in Fig. 2(b).

The simulation results for generating the 2.05 μm narrowband idler in DC-OPA is shown in Figs. 2(c) and 2(d). Figure 2(c) shows the output idler spectra under four different initial pump and signal chirps. It can be seen that the larger the input pump and signal chirps, the narrower the idler bandwidth. As shown in Fig. 2(d), the output idler's pulse duration is close to its transform-limited (TL) pulse duration, which is representative of all four cases. It is understandable that a larger pump and signal input chirp will lead to a narrower idler bandwidth because a longer idler pulse close to the transform limit always has a narrower spectrum bandwidth. The theoretical pump to idler conversion efficiency is around 20%, which results in a signal gain of 1.8×10^6.

4. EXPERIMENTAL RESULTS

The schematic DC-OPA setup is depicted in Fig. 3. The DC-OPA is pumped by a homemade 14-pass Ti:sapphire chirped-pulse amplification system, which produces 30 fs, up to 4 mJ pulses centered at 790 nm at 1 kHz repetition rate. In the experiment, the Ti:sapphire laser pulse energy of 1 mJ is used for the DC-OPA, which is split into two portions. A 5% portion of the 1 mJ beam passes through a neutral density filter and an iris diaphragm and is then focused onto a 3 mm thick sapphire plate to generate a stable single-filament continuum, which is the signal for seeding the DC-OPA. The signal is collimated by a lens and then passes through a 20.6 mm thick ZnSe plate with a positive dispersion of 10055 fs^2 at 1.28 μm. The 95% of the 1 mJ Ti:sapphire laser is the pump, which passes through a 45 mm thick SF57 plate with the same positive dispersion of 10055 fs^2 at 0.79 μm. A half-wave plate is inserted into the pump beam line to maintain orthogonal polarization between the pump and signal for Type I phase matching. A delay line allows the temporal overlap between the pump and the signal. A telescope is used to change the pump beam size on the BBO crystal. The BBO thickness is 15 mm with a type I phase-matching angle of 20°. A silicon plate is used to separate the signal and idler beams from the pump beam, and a 1.6 μm long-pass filter transmits the idler beam and blocks the signal beam.

It was confirmed by the numerical simulations that any chirp difference between the pump and the signal would widen the idler bandwidth. Thus, it is critical to maintain the same chirp rate between the pump and the signal. Even if the pump and seed pulse are chirped under the same GDD value, the chirp rates can be much different if their TL pulse durations are different. The TL pulse duration of the input pump

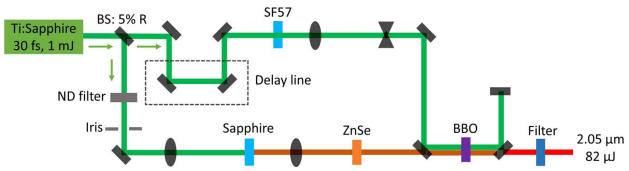

Fig. 3. Schematic setup of DC-OPA.

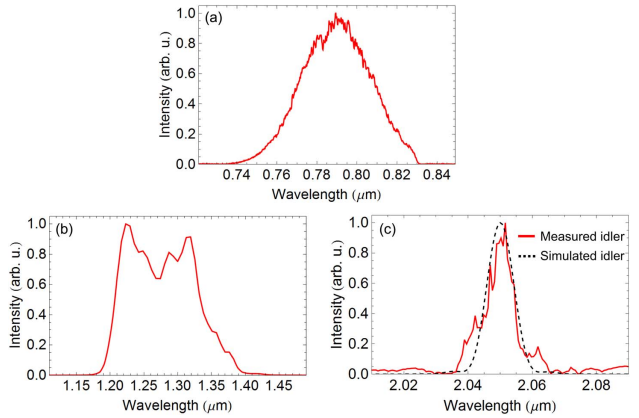

Fig. 4. (a) Input pump spectrum. (b) Output signal spectrum. (c) Measured output idler spectrum (solid red line) and simulated output idler spectrum (dotted black line).

spectrum is about 20 fs. The seed spectrum for the input signal is difficult to estimate from the entire broad seed spectrum generated by the white light generation (WLG), because only a small portion of the WLG spectrum is used in DC-OPA. However, the input signal spectrum can be roughly represented by the output signal spectrum, of which TL pulse duration is about 22 fs. Even though the TL pulse durations of the input pump and signal are close, many other optical components in the DC-OPA setup can give a different chirp rate. To fine-tune the chirp rate in the experiment, we fixed the ZnSe plate and slightly tilted the angle of the SF57 plate. At the same time, we monitored the idler bandwidth measured from the optical spectrum analyzer to find the narrowest idler bandwidth.

The experimental results are shown in Fig. 4. It can be seen that the signal and the idler spectrum bandwidths are close to the simulation results. The idler center wavelength can be easily tuned around 2.05 μm by changing the delay between the signal and the pump without any obvious decrease in efficiency, which is quite convenient to accommodate the gain spectrum from any Ho:YLF laser amplifier. The idler energy is around 82 μJ with an RMS single-shot stability of 1.5%, as shown in Fig. 5, while the pump single-shot stability is around 1%. The 2.05 μm near-field beam profile is shown in the inset picture in Fig. 5. The angular dispersion for the idler

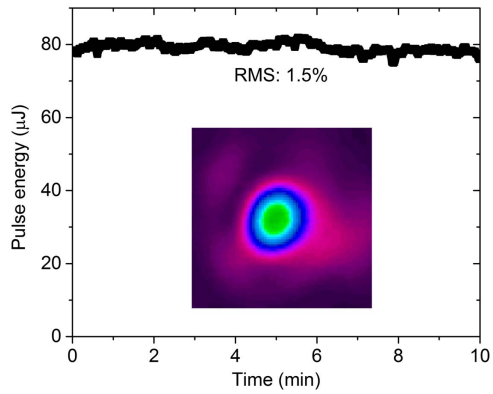

Fig. 5. Energy stability and beam profile (inset figure) of the idler.

was eliminated by using a collinear configuration between the pump and the signal. We are not concerned about the idler pulse duration because the idler will be used primarily for seeding an Ho:YLF laser. According to the simulations, the idler pulse duration is estimated to be around 1 ps. This high-energy, narrowband 2.05 μm pulse can be amplified to tens of mJ in a chirped-pulse Ho:YLF multipass amplifier.

5. CONCLUSION

We designed a DC-OPA using BBO crystal as the nonlinear media for generating narrowband 2.05 μm pulses, which are pumped by broadband Ti:sapphire laser pulses. We have experimentally generated 82 μJ narrowband 2.05 μm pulses with 1 mJ pump. The idler center wavelength can be easily tuned around 2.05 μm to accommodate the gain spectrum of any Ho:YLF laser amplifier by changing the delay between the signal and the pump. The bandwidth can be tuned by changing the input chirp of pump and signal. The high-energy narrowband 2.05 μm pulse will be an ideal source for seeding a Ho:YLF multipass amplifier, which allows easy synchronization when a Ti:sapphire laser and a Ho:YLF laser are needed for developing mid-IR laser pulses.

Funding. Air Force Office of Scientific Research (AFOSR) (FA9550-15-1-0037, FA9550-16-1-0013); Army Research Office (ARO) (W911NF-14-1-0383, W911NF-15-1-0336); Defense Advanced Research Projects Agency (DARPA) (W31P4Q1310017); National Science Foundation (NSF) (1506345).

Acknowledgment. Opinions, findings, and conclusions or recommendations expressed in this material are those of the authors and do not necessarily reflect the views of the NSF.

REFERENCES

1. Z. Chang and P. Corkum, "Attosecond photon sources: the first decade and beyond," J. Opt. Soc. Am. B **27**, B9–B17 (2010).
2. Z. Chang, P. B. Corkum, and S. R. Leone, "Attosecond optics and technology: progress to date and future prospects," J. Opt. Soc. Am. B **33**, 1081–1097 (2016).
3. Y. S. You, M. Wu, Y. Yin, A. Chew, X. Ren, S. Gholam-Mirzaei, D. A. Browne, M. Chini, Z. Chang, K. J. Schafer, M. B. Gaarde, and S. Ghimire, "Laser waveform control of extreme ultraviolet high harmonics from solids," Opt. Lett. **42**, 1816–1819 (2017).
4. K. Zhao, Q. Zhang, M. Chini, Y. Wu, X. Wang, and Z. Chang, "Tailoring a 67 attosecond pulse through advantageous phase-mismatch," Opt. Lett. **37**, 3891–3893 (2012).
5. B. Shan and Z. Chang, "Dramatic extension of the high-order harmonic cutoff by using a long-wavelength driving field," Phys. Rev. A **65**, 011804 (2001).
6. N. Ishii, K. Kaneshima, K. Kitano, T. Kanai, S. Watanabe, and J. Itatani, "Carrier-envelope phase-dependent high harmonic generation in the water window using few-cycle infrared pulses," Nat. Commun. **5**, 3331 (2014).
7. F. Silva, S. M. Teichmann, S. L. Cousin, M. Hemmer, and J. Biegert, "Spatiotemporal isolation of attosecond soft x-ray pulses in the water window," Nat. Commun. **6**, 6611 (2015).
8. J. Li, X. Ren, Y. Yin, Y. Cheng, E. Cunningham, Y. Wu, and Z. Chang, "Polarization gating of high harmonic generation in the water window," Appl. Phys. Lett. **108**, 231102 (2016).
9. T. Fuji, N. Ishii, C. Y. Teisset, X. Gu, T. Metzger, A. Baltuska, N. Forget, D. Kaplan, A. Galvanauskas, and F. Krausz, "Parametric amplification of few-cycle carrier-envelope phase-stable pulses at 2.1 μm," Opt. Lett. **31**, 1103–1105 (2006).
10. C. Vozzi, F. Calegari, E. Benedetti, S. Gasilov, G. Sansone, G. Cerullo, M. Nisoli, S. D. Silvestri, and S. Stagira, "Millijoule-level phase-stabilized few-optical-cycle infrared parametric source," Opt. Lett. **32**, 2957–2959 (2007).
11. C. Li, D. Wang, L. Song, J. Liu, P. Liu, C. Xu, Y. Leng, R. Li, and Z. Xu, "Generation of carrier-envelope phase stabilized intense 1.5 cycle pulses at 1.75 μm," Opt. Express **19**, 6783–6789 (2011).
12. O. D. Mücke, S. Ališauskas, A. J. Verhoef, A. Pugžlys, A. Baltuška, V. Smilgevičius, J. Pocius, L. Giniūnas, R. Danielius, and N. Forget, "Self-compression of millijoule 1.5 μm pulses," Opt. Lett. **34**, 2498–2500 (2009).
13. Y. Deng, A. Schwarz, H. Fattahi, M. Ueffing, X. Gu, M. Ossiander, T. Metzger, V. Pervak, H. Ishizuki, T. Taira, T. Kobayashi, G. Marcus, F. Krausz, R. Kienberger, and N. Karpowicz, "Carrier-envelope-phase-stable, 1.2 mJ, 1.5 cycle laser pulses at 2.1 μm," Opt. Lett. **37**, 4973–4975 (2012).
14. N. Ishii, K. Kaneshima, K. Kitano, T. Kanai, S. Watanabe, and J. Itatani, "Sub-two-cycle, carrier-envelope phase-stable, intense optical pulses at 1.6 μm from a BiB_3O_6 optical parametric chirped-pulse amplifier," Opt. Lett. **37**, 4182–4184 (2012).
15. K.-H. Hong, C.-J. Lai, J. P. Siqueira, P. Krogen, J. Moses, C.-L. Chang, G. J. Stein, L. E. Zapata, and F. X. Kärtner, "Multi-mJ, kHz, 2.1 μm optical parametric chirped-pulse amplifier and high-flux soft x-ray high-harmonic generation," Opt. Lett. **39**, 3145–3148 (2014).
16. N. Ishii, K. Kaneshima, T. Kanai, S. Watanabe, and J. Itatani, "Sub-two-cycle millijoule optical pulses at 1600 nm from a BiB_3O_6 optical parametric chirped-pulse amplifier," in *Conference on Lasers and Electro-Optics (CLEO)* (Optical Society of America, 2015), paper SF1M.3.
17. Y. Yin, J. Li, X. Ren, K. Zhao, Y. Wu, E. Cunningham, and Z. Chang, "High-efficiency optical parametric chirped-pulse amplifier in BiB_3O_6 for generation of 3 mJ, two-cycle, carrier-envelope-phase-stable pulses at 1.7 μm," Opt. Lett. **41**, 1142–1145 (2016).
18. Y. Fu, E. J. Takahashi, and K. Midorikawa, "High-energy infrared femtosecond pulses generated by dual-chirped optical parametric amplification," Opt. Lett. **40**, 5082–5085 (2015).
19. Y. Fu, E. J. Takahashi, Q. Zhang, P. Lu, and K. Midorikawa, "Optimization and characterization of dual-chirped optical parametric amplification," J. Opt. **17**, 124001 (2015).
20. Y. Fu, E. J. Takahashi, and K. Midorikawa, "Energy scaling of infrared femtosecond pulses by dual-chirped optical parametric amplification," IEEE Photon. J. **9**, 1–8 (2017).
21. B. E. Schmidt, N. Thir, M. Boivin, A. Larame, F. Poitras, G. Lebrun, T. Ozaki, H. Ibrahim, and F. Lgar, "Frequency domain optical parametric amplification," Nat. Commun. **5**, 3643 (2014).
22. J. Li, X. Ren, Y. Yin, K. Zhao, A. Chew, Y. Cheng, E. Cunningham, Y. Wang, S. Hu, Y. Wu, M. Chini, and Z. Chang, "53-attosecond x-ray pulses reach the carbon k-edge," Nat. Commun. **8**, 186 (2017).
23. G. Andriukaitis, T. Balčiūnas, S. Ališauskas, A. Pugžlys, A. Baltuška, T. Popmintchev, M.-C. Chen, M. M. Murnane, and H. C. Kapteyn, "90 GW peak power few-cycle mid-infrared pulses from an optical parametric amplifier," Opt. Lett. **36**, 2755–2757 (2011).
24. K. Zhao, H. Zhong, P. Yuan, G. Xie, J. Wang, J. Ma, and L. Qian, "Generation of 120 GW mid-infrared pulses from a widely tunable noncollinear optical parametric amplifier," Opt. Lett. **38**, 2159–2161 (2013).
25. S. Wandel, G. Xu, Y. Yin, and I. Jovanovic, "Parametric generation of energetic short mid-infrared pulses for dielectric laser acceleration," J. Phys. B **47**, 234016 (2014).
26. S. Wandel, M.-W. Lin, Y. Yin, G. Xu, and I. Jovanovic, "Parametric generation and characterization of femtosecond mid-infrared pulses in $ZnGeP_2$," Opt. Express **24**, 5287–5299 (2016).
27. D. Sanchez, M. Hemmer, M. Baudisch, S. L. Cousin, K. Zawilski, P. Schunemann, O. Chalus, C. Simon-Boisson, and J. Biegert, "7 μm, ultrafast, sub-millijoule-level mid-infrared optical parametric chirped pulse amplifier pumped at 2 μm," Optica **3**, 147–150 (2016).
28. P. Malevich, T. Kanai, H. Hoogland, R. Holzwarth, A. Baltuška, and A. Pugžlys, "Broadband mid-infrared pulses from potassium titanyl

arsenate/zinc germanium phosphate optical parametric amplifier pumped by Tm, Ho-fiber-seeded Ho:YAG chirped-pulse amplifier," Opt. Lett. **41**, 930–933 (2016).
29. Y. Yin, J. Li, X. Ren, Y. Wang, A. Chew, and Z. Chang, "High-energy two-cycle pulses at 3.2 μm by a broadband-pumped dual-chirped optical parametric amplification," Opt. Express **24**, 24989–24998 (2016).
30. Y. Yin, A. Chew, X. Ren, J. Li, Y. Wang, Y. Wu, and Z. Chang, "Towards terawatt sub-cycle long-wave infrared pulses via chirped optical parametric amplification and indirect pulse shaping," Sci. Rep. **8**, 45794 (2017).
31. G. Xu, S. Wandel, and I. Jovanovic, "Nondegenerate parametric generation of 2.2-mJ, few-cycle 2.05-μm pulses using a mixed phase matching scheme," Rev. Sci. Instrum. **85**, 023102 (2014).
32. K. Murari, H. Cankaya, P. Kroetz, G. Cirmi, P. Li, A. Ruehl, I. Hartl, and F. X. Kärtner, "Intracavity gain shaping in millijoule-level, high gain Ho:YLF regenerative amplifiers," Opt. Lett. **41**, 1114–1117 (2016).
33. Q. Zhang, E. J. Takahashi, O. D. Mücke, P. Lu, and K. Midorikawa, "Dual-chirped optical parametric amplification for generating few hundred mJ infrared pulses," Opt. Express **19**, 7190–7212 (2011).
34. Y. Fu, E. Takahashi, B. Xue, and K. Midorikawa, "Generation of a 200-mJ class infrared femtosecond laser by dual-chirped optical parametric amplification," in *Conference on Lasers and Electro-Optics (CLEO)*, OSA Technical Digest (online) (Optical Society of America, 2017), paper SM3I.3.
35. S. Wandel, M.-W. Lin, Y. Yin, G. Xu, and I. Jovanovic, "Bandwidth control in 5 μm pulse generation by dual-chirped optical parametric amplification," J. Opt. Soc. Am. B **33**, 1580–1587 (2016).
36. Z. Hong, Q. Zhang, S. A. Rezvani, P. Lan, and P. Lu, "Tunable few-cycle pulses from a dual-chirped optical parametric amplifier pumped by broadband laser," Opt. Laser Technol. **98**, 169–177 (2018).
37. M. Hemmer, D. Sánchez, M. Jelínek, V. Smirnov, H. Jelinkova, V. Kubeček, and J. Biegert, "2-μm wavelength, high-energy Ho:YLF chirped-pulse amplifier for mid-infrared OPCPA," Opt. Lett. **40**, 451–454 (2015).
38. L. von Grafenstein, M. Bock, D. Ueberschaer, U. Griebner, and T. Elsaesser, "Ho:YLF chirped pulse amplification at kilohertz repetition rates-4.3 ps pulses at 2 μm with GW peak power," Opt. Lett. **41**, 4668–4671 (2016).
39. Y. C. Yin, D. French, and I. Jovanovic, "Ultrafast temporal pulse shaping via phase-sensitive three-wave mixing," Opt. Express **18**, 18471–18482 (2010).
40. Y. R. Shen, *The Principle of Nonlinear Optics* (Wiley, 2003).
41. M. D. Feit and J. A. Fleck, "Computation of mode properties in optical fiber waveguides by a propagating beam method," Appl. Opt. **19**, 1154–1164 (1980).